













Evidence of Magnetic Reconnection in Ganymede's Wake Region From Juno

Special Collection:

Io and the Galilean Satellites

J. Joseph¹ , W. S. Kurth¹ , A. H. Sulaiman² , J. E. P. Connerney³ , F. Allegrini^{4,5} , S. Duling⁶ , G. Clark⁷ , J. B. Faden¹, C. W. Piker¹, A. N. Jaynes¹ , B. H. Mauk⁷ , and S. J. Bolton⁴ 

Key Points:

- Juno passed near a magnetic reconnection X-line in Ganymede's downstream region on 7 June 2021
- Juno Waves observations provide a positive indication of being in the reconnection separatrix site
- Juno JADE electron measurements show the flux increase and pitch angle distributions expected in a separatrix region

¹University of Iowa, Iowa, IA, USA, ²University of Minnesota, Minneapolis, MN, USA, ³University of Maryland, College Park, MD, USA, ⁴Southwest Research Institute, San Antonio, TX, USA, ⁵University of Texas, San Antonio, TX, USA, ⁶Institute of Geophysics and Meteorology, University of Cologne, Köln, Germany, ⁷JHU/Applied Physics Laboratory, Laurel, MD, USA

Correspondence to:

J. Joseph,
jayasri-joseph@uiowa.edu

Citation:

Joseph, J., Kurth, W. S., Sulaiman, A. H., Connerney, J. E. P., Allegrini, F., Duling, S., et al. (2024). Evidence of magnetic reconnection in Ganymede's wake region from Juno. *Journal of Geophysical Research: Space Physics*, 129, e2024JA033173. <https://doi.org/10.1029/2024JA033173>

Received 12 AUG 2024

Accepted 15 NOV 2024

Author Contributions:

Conceptualization: J. Joseph
Data curation: J. Joseph, J. B. Faden, C. W. Piker
Formal analysis: J. Joseph
Funding acquisition: W. S. Kurth
Investigation: J. Joseph
Methodology: J. Joseph
Project administration: W. S. Kurth
Resources: J. Joseph, W. S. Kurth, J. E. P. Connerney, F. Allegrini, S. Duling, G. Clark, B. H. Mauk, S. J. Bolton
Software: J. Joseph
Supervision: W. S. Kurth
Validation: J. Joseph, A. H. Sulaiman
Visualization: J. Joseph, A. H. Sulaiman, F. Allegrini, S. Duling, G. Clark, J. B. Faden, C. W. Piker
Writing – original draft: J. Joseph

© 2024 The Author(s).

This is an open access article under the terms of the [Creative Commons Attribution-NonCommercial License](https://creativecommons.org/licenses/by-nc/4.0/), which permits use, distribution and reproduction in any medium, provided the original work is properly cited and is not used for commercial purposes.

Abstract Magnetic reconnection has been commonly reported between the solar wind IMF and the magnetic field of Earth and other planets. A similar phenomenon is expected between Jupiter's magnetosphere and Ganymede's mini magnetosphere inside the Jovian magnetosphere. This article is the first report of a reconnection event in the tail region of Ganymede. We present compelling evidence that Juno flew in close proximity to an X-line, that was not within the tail current sheet, but rather in the turbulent wake area of Ganymede. We report the observation of distinctive electron Bernstein mode waves with unique characteristics particular to a separatrix region of the reconnection site. We detect a clear reversal of a magnetic field component. Electron densities and pitch angle distributions also indicate that Juno possibly traversed the inflow, and outflow region surrounding the separatrix region. Finally, from the time sequence of the observations by the different instruments on Juno, we reconstruct a likely trajectory of Juno around the reconnection site.

1. Introduction

Jupiter's moon Ganymede is the only known satellite to have a magnetosphere of its own within a planetary magnetosphere (Gurnett et al., 1996; Kivelson et al., 1996). The dipole fields of Ganymede and Jupiter are oriented in nearly opposite directions (Kivelson et al., 2002). The plasma interaction between Ganymede and Jupiter is comparable to some extent to that of Earth and the Sun under a southward interplanetary magnetic field. However, due to the sub-Alfvénic speed of the plasma flow Alfvén wing interactions in the wake region of Ganymede are likely (Burkholder et al., 2024). Some proof of magnetic reconnection near the upstream magnetopause of Ganymede is given in Ebert et al. (2022) and Romanelli et al. (2022). Collinson et al. (2018) reported reconnection-generated fast flows near the flank magnetopause of Ganymede from the PLS data from the Galileo G1 flyby. Reconnection at Ganymede's downstream has not been reported until now. MHD simulations of Ganymede's magnetosphere predict magnetic reconnections both at the magnetopause and magnetotail (Dorelli & Birn, 2003; Dorelli et al., 2015; Fatemi et al., 2016; Jia & Kivelson, 2021; Karimabadi et al., 2011). The conditions for reconnection at Ganymede are highly favorable compared to Earth and Jupiter (Masters, 2017; Paschmann et al., 2013), indicating considerable reconnection rates at all Ganymede magnetopause locations. Even though not directly calculated, a significant reconnection rate in the magnetotail is expected to satisfy the magnetic flux conservation (Kaweeyanun et al., 2020). Numerous studies of the reconnection process at Earth's magnetopause and magnetotail help us understand how reconnection may proceed in other systems, including at Ganymede, where observations are scarce.

Magnetic reconnection in plasma refers to a microscopic process in which oppositely directed components of magnetic field lines in close proximity break and reconnect to the neighboring field line. The abrupt reconfiguration of magnetic field lines causes the violation of the ideal plasma frozen-in condition. When a charged particle sees a varying magnetic field within the particle's gyro radius, the particle becomes decoupled from the field. Ions with a larger gyro radius than electrons get decoupled from the field before the electrons. The difference between decoupled electron and ion motions gives rise to a Hall current (Sonnerup, 1979; Terasawa, 1983). The Hall effect is essential for fast reconnection rates in collisionless plasmas (Birn et al., 2001; Dorelli et al., 2015). A large amount of magnetic energy is released during the topological restructuring of magnetic fields (Biskamp, 2000). The local explosive process creates turbulent regions in plasma. Plasma that is accelerated by magnetic reconnection forms exhausts causing the generation of sharp gradients in phase space at

Writing – review & editing: W. S. Kurth,
A. H. Sulaiman, S. Duling, A. N. Jaynes

the boundaries. So, close to the reconnection site, various plasma waves, such as upper hybrid, Langmuir, electron cyclotron harmonic (ECH), broadband electrostatic solitary waves along with lower hybrid and whistler mode waves (Khotyaintsev et al., 2019) are generated to relax such gradients.

The study of reconnection events is challenging because of their small spatial dimension compared to the plausible occurrence region and their intermittent manifestation. Special effort has been put into studying the reconnection events near Earth by Cluster (Escoubet et al., 2001), THEMIS (Angelopoulos, 2008), and Magnetospheric Multiscale (MMS) (Burch et al., 2016) missions. Studies on Earth have found that the occurrence of certain waves like Langmuir, ECH, and electrostatic solitary waves (Viberg et al., 2013) could act as a distinct marker for a reconnection site. It is often not possible to identify such distortions in real/phase space from particle data due to insufficient temporal resolutions of particle measurements. However, magnetic reconnection is often assumed from the observations of heated and accelerated thermal and suprathermal electron flows (e.g., Ebert et al., 2017; Fuselier et al., 2014; Phan et al., 2013).

Even with sophisticated instrumentation the study of reconnection events is found to be difficult in Earth's magnetosphere. The problem increases in the case of Ganymede as we only have sparse observations by two satellites. On 7 June 2021, Juno was the first spacecraft to fly through the Ganymede's magnetotail ($z = 0$) at an altitude of $\sim 2.9 R_G$ or 7,668 km ($x = 2.67 R_G$ or 7,033 km, $y = -1.16 R_G$ or $-3,055$ km), where R_G is the radius of Ganymede (2,634 km). In this study, we report for the first time a magnetic reconnection around Ganymede's magnetotail at $x = 3.06 R_G$, $y = -1.62 R_G$, $z = -0.14 R_G$ during the close flyby. Measurements from Waves, particles, and magnetic field instruments point to Juno's proximity to an X-line. However, we must make allowance for the fact that instruments on Juno are inadequate for any detailed study of reconnection physics. In Section 2, we describe the observations of the reconnection event as seen by the various instruments on Juno. These observations are analyzed in Section 3. We summarize our findings in Section 4.

2. Observations

On 7 June 2021, the Juno mission had an opportunity to examine Ganymede's magnetospheric activities during a close flyby. Juno approached Ganymede from the downstream side and left through the upstream side (Allegrini et al., 2022; Clark et al., 2022; Hansen et al., 2022; Kurth et al., 2022). Figure 1 shows Juno's trajectory overlaid on an MHD magnetic field model (Duling et al., 2022). Here we use the Ganymede centric (GPhiO) coordinate system, where z is parallel to Jupiter's rotation axis, y approximately points toward Jupiter and x completes the right-handed system, along corotation. The approximate position of Juno at 16:48:37 UT, where the downstream reconnection event reported in this study occurred, is marked. The following subsections describe the distinctive observations by different instruments on Juno around the reconnection event.

2.1. Plasma Waves

For this study, measurements of electric and magnetic fields were obtained from the Waves instrument (Kurth et al., 2017). We use the low-frequency receivers, which operate in the frequency range of 50 Hz to 20 kHz. The most compelling evidence of Juno's passing over a magnetic reconnection separatrix is obtained from this instrument. The sampling rate of this receiver is 50 kHz (20 microseconds), which is high enough to observe the electron scale structures. But it is to be noted that the high-resolution waveform data are available to us for at the most ~ 123 milliseconds (6,144 samples) in every second. Reduced resolution continuous observation from this instrument uses an onboard FFT engine that transmits binned FFT results once a second in 18 logarithmically selected channels. Here we use the full-resolution burst waveform to identify the fine structures. The high-resolution frequency spectrum in this study is calculated on the ground from the time domain burst data using blocks of 1,024 samples. Figure 2 shows the time and frequency domain data in the region of the reconnection event. A very strong ECH wave with multiple harmonics at ~ 1 kHz spacing is clearly seen in panels A1 and B1 (zoomed in). The time domain waveform in panel B2 also shows the baseline being modulated by ECH waves. A large negative voltage peak of ~ 80 mV is seen at 16:48:37.620 UT (Figures 2a2, 2b2) indicating an electrostatic solitary wave (ESW).

2.2. Charged Particles

Particle data from the JADE instrument (Allegrini et al., 2022; McComas et al., 2017), specifically the JADE-E sensors that measure electrons in the energy range of ~ 0.030 –32 keV, are used to examine the thermal/suprathermal electron behavior during the reconnection event. Measurements of electron flux and pitch angles are binned

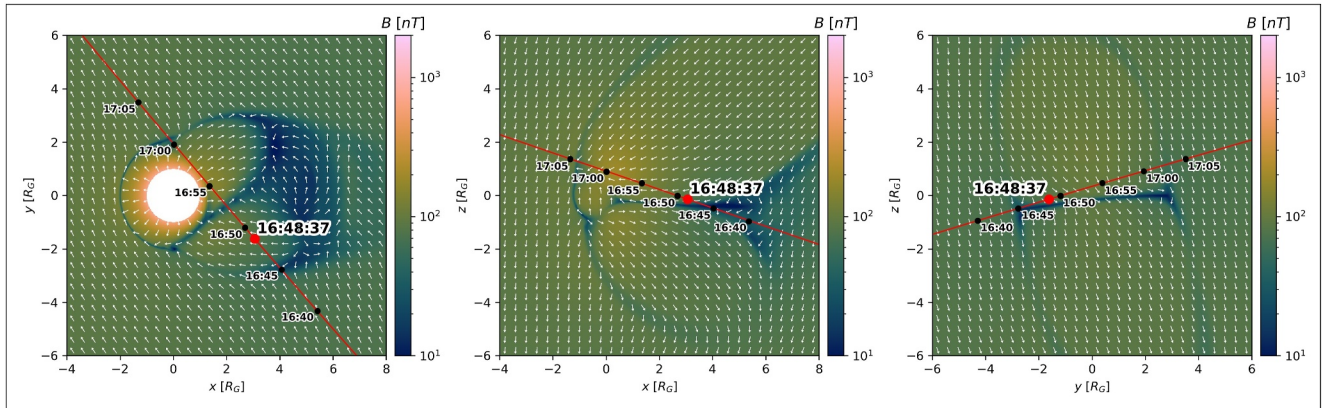


Figure 1. Projected Juno trajectory (red lines) on the magnetic field model (Duling et al., 2022) in reference to the reconnection event at $(3.06 R_G, -1.62 R_G, -0.14 R_G)$. From left to right are the views of the x - y ($z = -0.14 R_G$), x - z ($y = -1.62 R_G$), and y - z ($x = 3.06 R_G$) planes, respectively. Juno's position around the reconnection event is marked by the red circles. Some other times are also shown (black dots) for reference.

for one second as JADE-E sensors step through different energies. One-second scans of the binned electron (0.030–32 keV) flux versus time (Panel B) and corresponding pitch angles for suprathermal electrons (200–600 eV) (Panel A) are shown in Figure 3. We focus on the suprathermal electrons as they are expected to have the most distinctive pitch angle distributions (PADs) close to the reconnection site. However, JADE had limited coverage of pitch angle measurements at this time. The type of PAD is presumed by visual inspection. A closer examination of Figure 3A shows a monotonically decreasing electron flux from $\sim 30^\circ$ to 90° pitch angles that resembles a field-aligned distribution at 16:48:36–16:48:38 UT. But by looking at $\sim 120^\circ$ – 150° pitch angles during 16:48:36–16:48:37 UT, we also see the presence of some isotropic PAD. A change in the trend from a moderately field-aligned to a jet-like highly field-aligned distribution during $\sim 16:48:37$ – $16:48:38$ UT is worth noting. Observations of high-energy

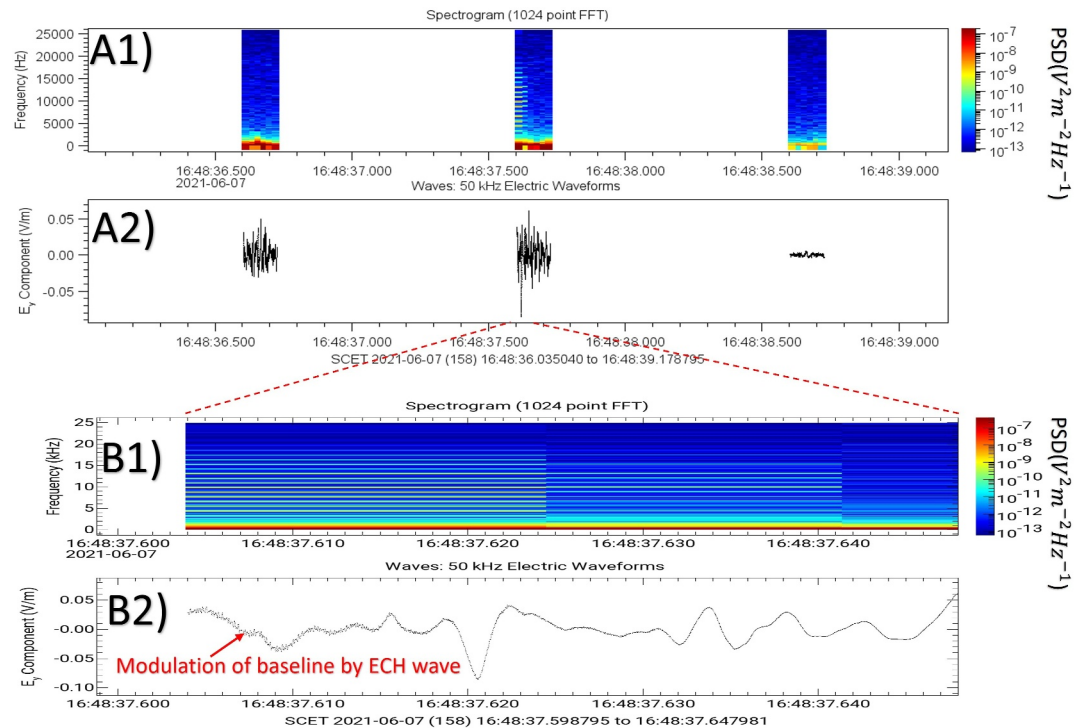


Figure 2. Electric field observation around the reconnection event. Panels (a2 and b2) (zoomed in) show the electric field recorded by the electric dipole antenna. The resulting spectrogram of the electric field derived by blocks of 1,024-point FFT is shown in panels (a1 and b1) (zoomed in).

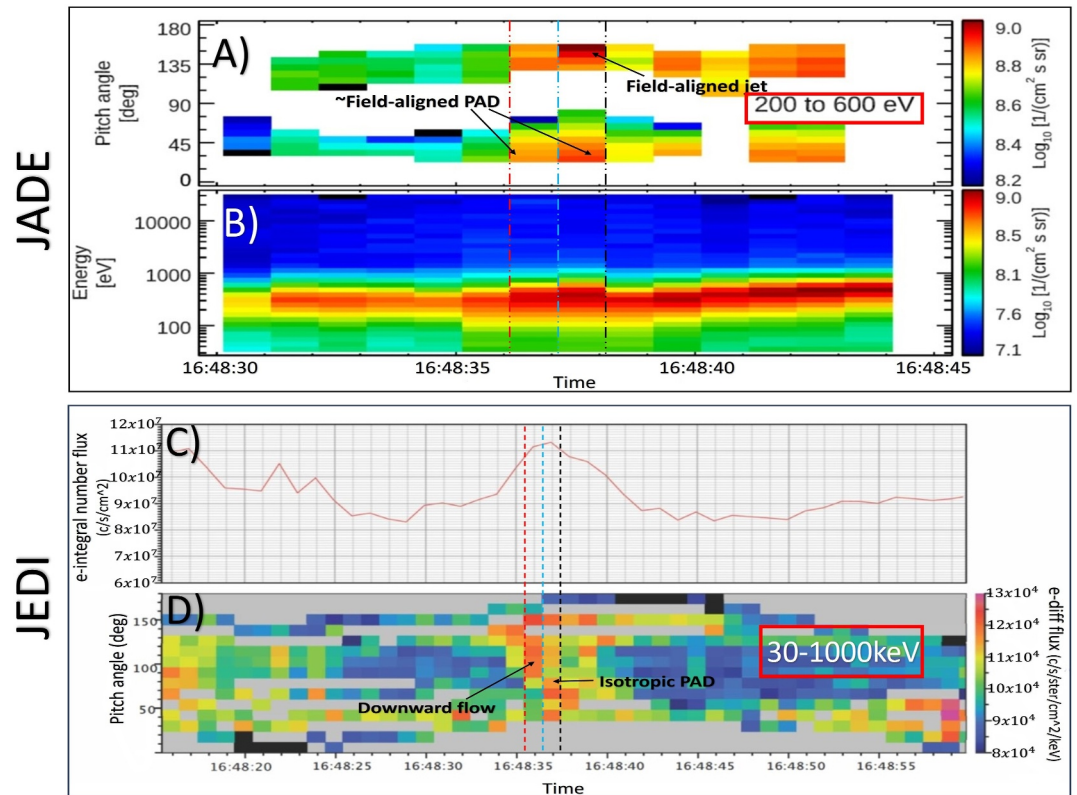


Figure 3. Electron characteristics seen by JADE and JEDI around the reconnection event. Panels (a and b) show the binned electron pitch angle and flux recorded by JADE, respectively. Regions around the reconnection event are indicated by the dash-dotted lines. Panels (c and d) show the integral number flux and pitch angles of electrons seen by JEDI, respectively. Regions around the reconnection event are marked by the dashed lines.

(30–1,000 keV) electrons from the JEDI instrument (Clark et al., 2022; Mauk et al., 2017) are also included (Figures 3c and 3d) to get a complete picture. Though less clear, a change in electron flux and pitch angle behavior is also seen in high-energy (30–1,000 keV) electrons around the reconnection site. Pitch angle distributions of electrons around the reconnection site are quite complex and depend on the energy (Li et al., 2022). Øieroset et al. (2002) found that the fluxes of energetic electrons up to ~ 300 keV peak near the center of the diffusion region. They also show that the electron PAD is field-aligned bidirectional at energies below ~ 2 keV and becomes isotropic above ~ 6 keV. Other studies demonstrate that outside the diffusion region, as seen from the observations at Earth, the inflow region generally contains cold plasma with mostly field-aligned electron distributions with equal electron flux in parallel and antiparallel directions (Borg et al., 2012; Viberg et al., 2013). The ion outflow (exhaust) regions contain suprathermal electrons with primarily isotropic (flat top) electron PAD (Asano et al., 2008; Borg et al., 2012). Reconnection accelerates particles inside the separatrix region and jets of suprathermal electrons flow along the separatrix. From Figure 3A, we see an increased flux of suprathermal electrons (200–600 eV) with likely field-aligned distribution during $\sim 16:48:36$ – $16:48:38$ UT. An unidirectional jet-like structure is evident during $\sim 16:48:37$ – $16:48:38$ UT. High energy electrons (Figure 3C & D) in the range of 30–1,000 keV also show flux increase at $\sim 16:48:35.5$ – $16:48:37.5$ UT. The PAD is assumed to be isotropic at $16:48:36.5$ – $16:48:37.5$ UT (Figure 3D), as the electron flux does not show a clear bias toward any specific pitch angles. The PAD is more directional ($>90^\circ$) at $16:48:35.5$ – $16:48:36.5$ UT. Considering the small size of electron diffusion region and low sampling rate of Juno's particle data, particle observations around the reconnection site may include samples from adjacent regions.

2.3. Magnetic Field

We use high-resolution (64 Hz) measurements from Juno's fluxgate magnetometer (FGM) (Connerney et al., 2017) for determining the background magnetic field (Figure 4a). A zoomed in view near the event is shown

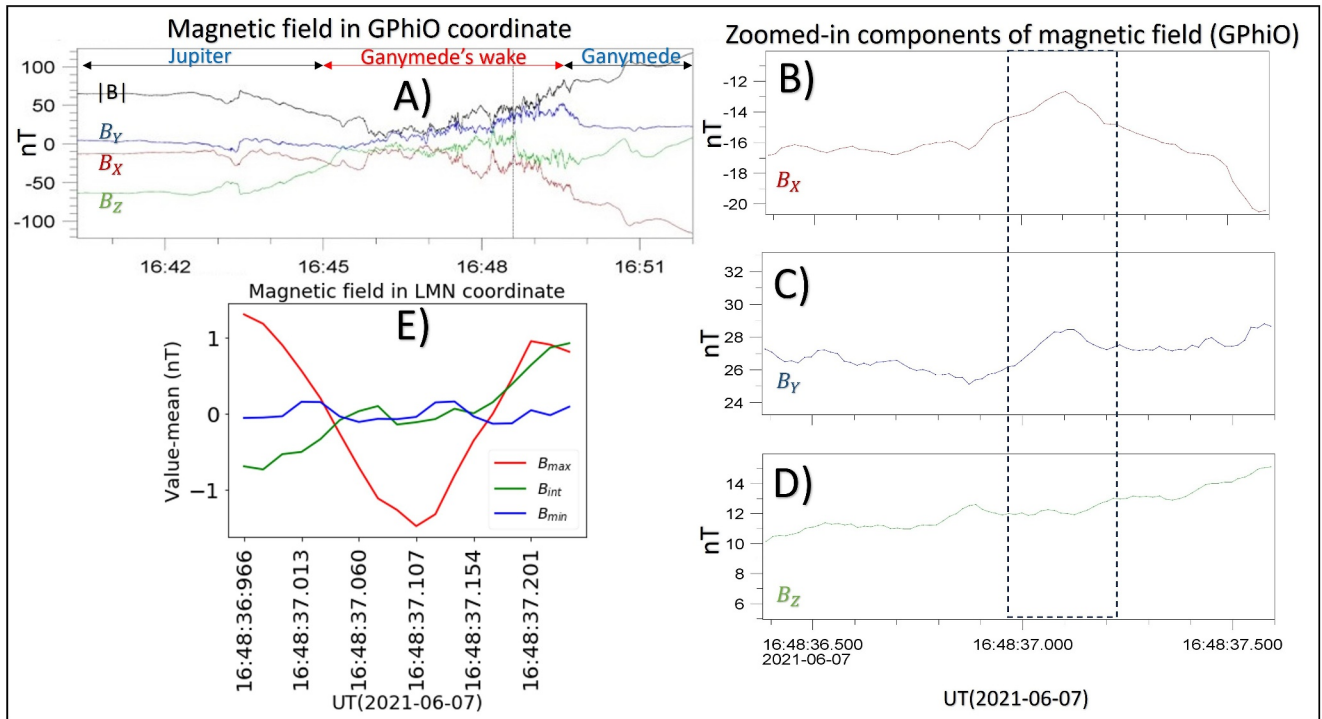


Figure 4. Background magnetic field. Panel (a) shows the variation in magnetic field in GPhiO coordinates. Magnetic boundaries are shown on top (Clark et al., 2022). The vertical dashed line in panel (a) shows the time of the reconnection event. Panels (b), (c), and (d) are the zoomed-in view of the X, Y, and Z components of the magnetic field around the event. Region of interest around the reconnection is marked by the dashed rectangle. Panel (e) shows the components of the magnetic field in LMN coordinates. B_{max} , B_{int} and B_{min} are the variations in magnetic fields in the maximum, intermediate, and minimum variance directions obtained from the Minimum Variance Analysis.

in Figures 4b–4d as a function of time in GPhiO coordinates. A considerable disturbance in the magnetic field is seen around the reconnection. Through the turbulent region, magnetic field components changed from a B_z -dominated orientation in Jupiter's magnetosphere to a B_x/B_y -dominant configuration in Ganymede's magnetosphere. It is to be noted that to visualize the behavior of the magnetic field relating to reconnection a coordinate transformation is needed (Figure 4e) which is described later (Section 3.3).

3. Discussion

3.1. Wave Data Analysis

In the separatrix region close to the electron diffusion region (EDR), waves covering a broad range of frequencies specifically, Langmuir, upper hybrid, ESWs, and ECH waves are seen (Retinó et al., 2006; Vaivads et al., 2004). They act as indirect markers for a nearby x-line. As evident from Figures 2a1, 2b1 and 5a, we observed very strong ECH waves with many (4th–12th) harmonics in the range of ~4–16 kHz. Unexpectedly the lower (1st–3rd) harmonics of the ECH waves are missing. This specific feature makes the observed ECH waves stand apart from the normal ECH waves category (Hubbard et al., 1979). Based on MMS observations we suspect these ECH waves are generated by the ring/crescent shaped electron distribution of suprathermal electrons. We calculated the lower limit of f_{pe} (39.782 kHz) from JADE partial electron density data. Wave powers for these ECH waves are concentrated at frequencies (4–16 kHz) much below f_{pe} (>39 kHz), ruling out the possibility of upper hybrid oscillations misinterpreted as ECH waves.

Reconnection phenomena are well studied in the Sun-Earth system. Similar distinguishing strong ECH waves were observed by MMS (Li et al., 2020) near the EDR at Earth's subsolar magnetopause on 24 December 2016. Thermalized electron outflows were determined to be the source of the ECH waves in this case. Their analysis showed that ECH waves were generated due to the crescent-shaped agyrotropic electron distributions of the outflowing electrons around the EDR. Numerical simulation (Umeda, 2007) shows that if thermal electrons are responsible for the ring/crescent-shaped distribution, lower harmonics of the ECH waves will be weak or absent.

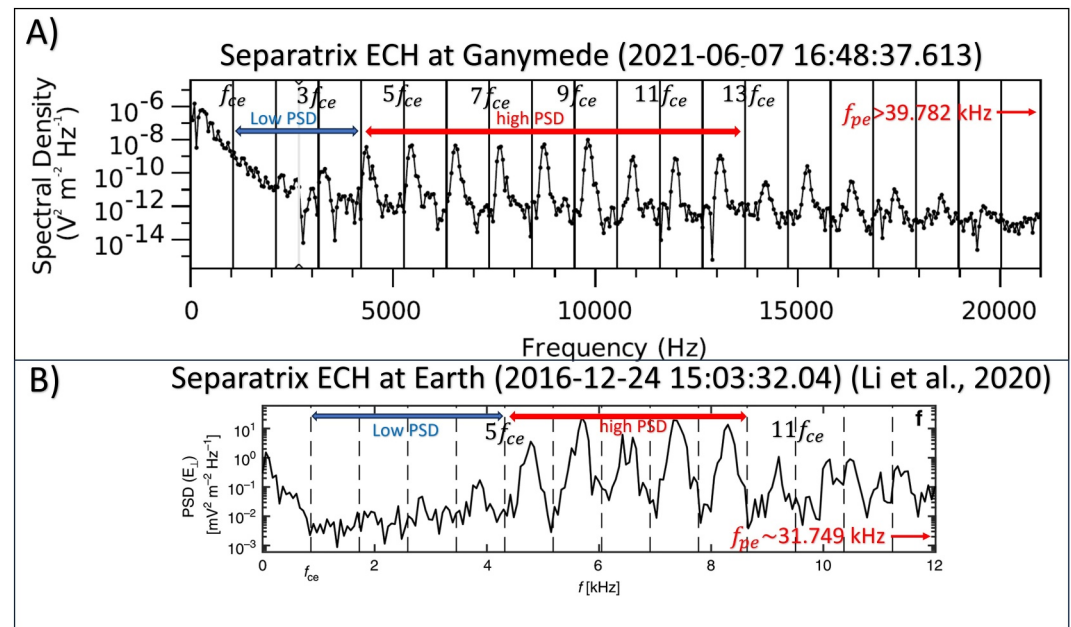


Figure 5. Power spectral densities (PSDs) of the characteristic electron cyclotron harmonic (ECH) waves found near the reconnection sites. Panel (a) shows the PSD of ECH waves with wave power concentrated between the 4th to 12th harmonic bands for the Ganymede downstream reconnection. Panel (b) is for comparison with a similar observation at Earth. Panel (b) is reproduced from Figure 4f in Li et al. (2020). In the case of Earth, wave powers are concentrated between the 5th to 9th harmonic bands. In both cases, lower harmonics of ECH waves are weak/absent.

This is in sharp contrast to the common ECH waves seen in the equatorial region of the planet's magnetosphere. Figure 5A shows a snapshot (at 16:48:37.613 UT) of the power spectral density of the ECH waves encountered by Juno near the EDR in Ganymede's downstream region. Compare this with the MMS observation near the EDR at Earth's magnetopause (Figure 5b) and note the missing lower harmonics. Missing lower harmonics of ECH waves indirectly indicates an underlying ring/crescent-shaped distribution of suprathermal electrons rather than hot electrons (Umeda, 2007). A ring/Crescent-shaped distribution of suprathermal electrons is an important indicator of proximity to an EDR (e.g., Fuselier et al., 2017; Webster et al., 2018). Unlike MMS, Juno particle instruments are not designed to measure such electron distributions directly. But the characteristic ECH waves with missing lower harmonics provide evidence for a separatrix region close to the EDR containing such an electron distribution. The Juno electric field instrument also recorded a strong (~80 mV) ESW at 16:48:37.620 UT (Figures 2a2, and 2b2). ESWs are often reported in the magnetotail (Cattell et al., 2005; Deng et al., 2004; Khotyaintsev et al., 2010) and at the magnetopause (Retinó et al., 2006) reconnection regions of Earth.

3.2. Particle Data Analysis

The electron motions in the inflow and the outflow regions of a reconnection site are well studied at Earth by the Cluster and MMS missions. A statistical study by Borg et al. (2012) and other case studies (Asano et al., 2008; Chen et al., 2008; Egedal et al., 2005, 2010; Nagai et al., 2001) show that the electron distribution in the inflow region and the outflow region is mostly field-aligned and isotropic, respectively. The distribution of suprathermal electrons in the separatrix region is field-aligned (Eriksson et al., 2018; Nan et al., 2022). JADE had partial pitch angle coverage available surrounding the reconnection event. From the trend of the electron distributions, we see indications of bidirectional field-aligned and field-aligned distribution with a jet-like structure of suprathermal electrons during ~16:48:36–16:48:37 UT and ~16:48:37–16:48:38 UT, respectively (Figure 3a). These observations suggest that Juno was in the inflow/outflow region followed by the separatrix region. We also see an increase in electron flux with isotropic PAD in high-energy populations (30–1,000 keV) during the time interval (~16:48:36.5–16:48:37.5 UT) marked by the blue and black dashed lines in Figures 3C and 3D. This behavior implies that Juno was at the outflow region at that time. Just before this, at the time interval between the red and blue dashed lines (~16:48:35.5–16:48:36.5 UT) in Figure 3d, an increased flow of high-energy electrons toward the reconnection site (refer to Section 3.3) is visible as expected in an inflow region.

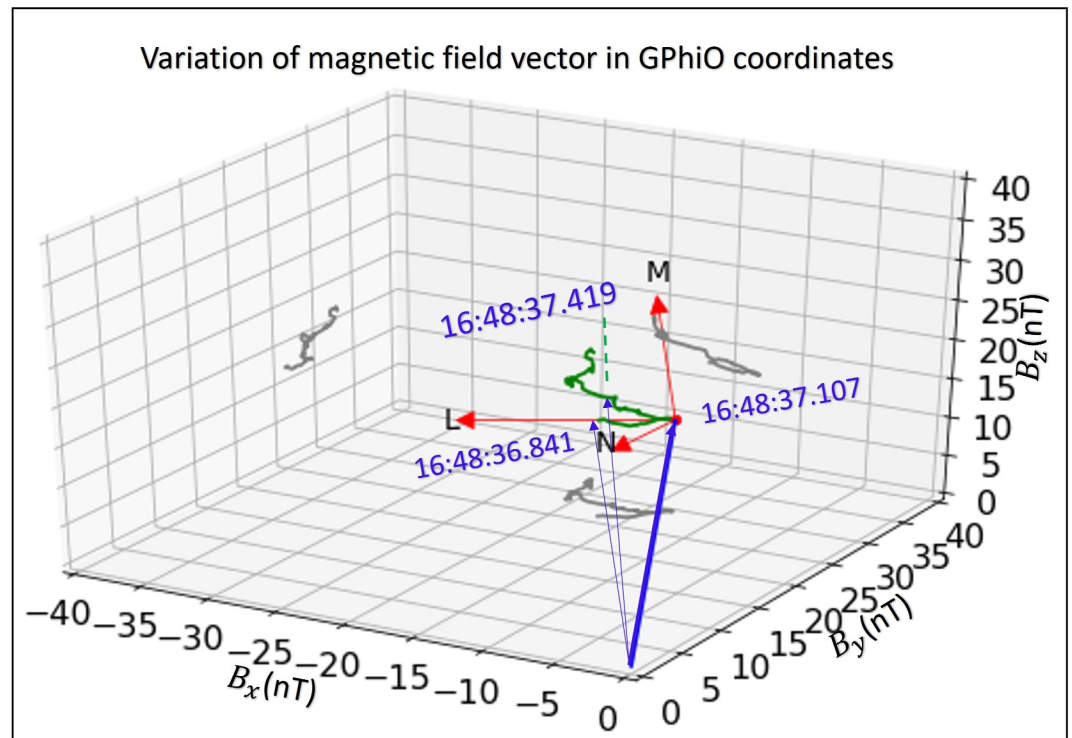


Figure 6. 3D view of the variation in magnetic field vector in GPhiO coordinates. The blue arrows show the magnetic field vectors at three time instances around the reconnection. The green curve shows the trajectory of the head of the vector. The projections of the vector variations are shown by the gray curves. The orientation of the LMN coordinates as derived by the Minimum Variance Analysis with respect to the GPhiO coordinates is shown in red.

3.3. Magnetic Field Analysis

The planetocentric coordinate system used in spacecraft measurement is mostly not aligned with the reconnection plane. Therefore, to identify reconnection a transformation of the coordinate system is required. In a suitable cartesian coordinate system, the reconnection plane contains a L-axis along which the component of the magnetic field changes the most and an N-axis, perpendicular to the current sheet. The third M-axis completes the right-handed orthogonal coordinate system.

To identify the reversal of magnetic field, the Minimum Variance Analysis (MVA) method (Sonnerup & Cahill, 1967) is used in this study. The variance matrix indicates the directions of the highest variance (L or B_{\max}), the intermediate variance (M or B_{int}), and the lowest variance (N or B_{\min}). In the wake region of Ganymede, the background magnetic field was very turbulent (Figure 4a), making the magnetic field analysis challenging. Most reconnection phenomena observed at Earth are laminar; but some turbulent reconnections are also seen (Ergun et al., 2022). For a targeted analysis of the event, 18 samples around the local magnetic field peak as shown by the dashed rectangle in Figures 4b–4d, are used. The variations of the magnetic components in B_{\max} , B_{int} , B_{\min} are plotted in Figure 4e. In our study, maximum to intermediate (λ_1/λ_2) and intermediate to minimum (λ_2/λ_3) eigenvalue ratios are 3.83 and 22.69, respectively. Generally, for magnetic reconnection, the three eigenvalues of the variance matrix are expected to be distinct. However, there are a significant number of cases where the lowest variance stands out, but the highest and intermediate variance have similar values. So, any pair of vectors lying in the plane perpendicular to B_{\min} , may serve as B_{\max} and B_{int} . In our case even though the λ_1/λ_2 value is moderate (3.83), we can still use MVA for normal-vector and normal-field-component determinations, as $\lambda_3 \ll \lambda_2 - \lambda_1$ (Paschmann & Daly, 1998). A value of $\lambda_1/\lambda_2 > 5$ (Romanelli et al., 2022) is required for the MVA analysis to produce a deterministic estimation of B_{\max} , B_{int} . In our case, λ_1/λ_2 being 3.83, B_{\max} , B_{int} are not well defined. A future study could cover a detailed analysis of the magnetic field using other methods. From the current analysis, we see a reversal of the magnetic field (B_{\max} component) at 16:48:37.107 UT. Figure 6 shows the variation of the magnetic field vector in GPhiO coordinates around the reconnection event in three dimensions. The orientation of

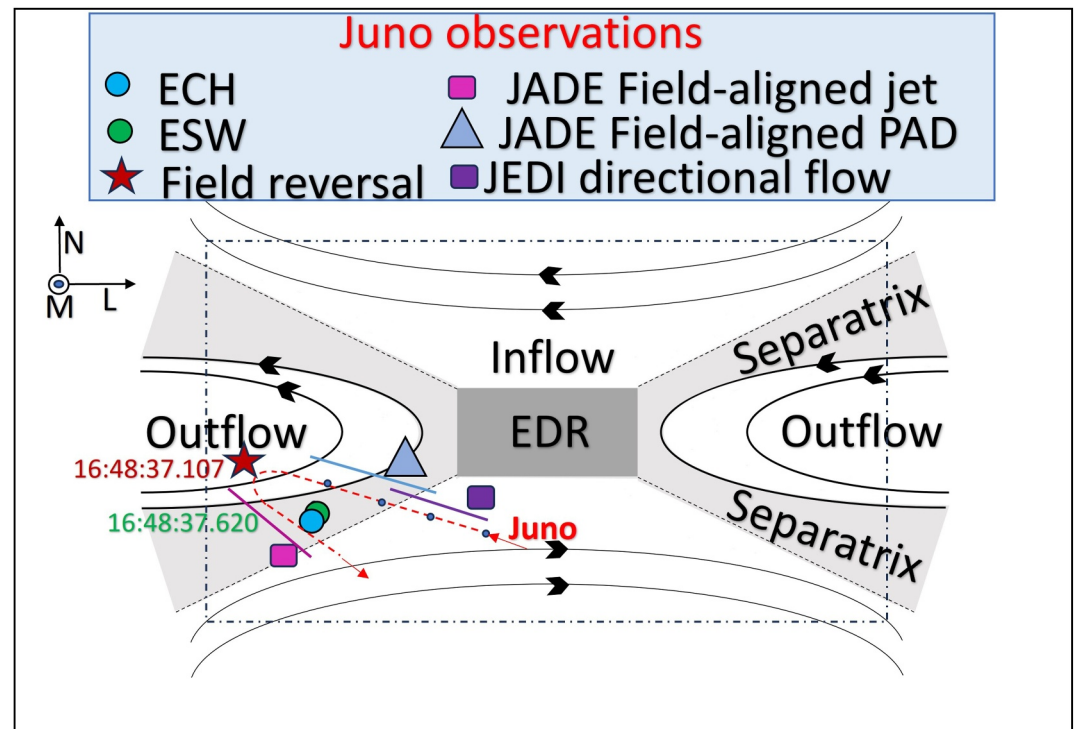


Figure 7. Illustration of sequence of observations by various instruments on Juno. Red arrows show the Juno trajectory. Circles are used to mark the plasma waves in the separatrix region. A star is used to mark the time of the reversal of the magnetic field. Waves and the magnetic field measurements had a sampling resolution of 50 kHz and 64 Hz, respectively. The rectangles and the triangle are used to indicate different pitch angle distributions of electrons as observed by JADE and JEDI. The temporal resolution of the particle data used here is of the order of one second.

LMN coordinates as determined by the MVA with respect to GPhiO coordinates is shown in the figure inset. We notice that in this configuration, the reconnection plane is only slightly offset from the X-Y plane of the GPhiO coordinates.

3.4. Combined Observations

Juno encountered ECH emissions in high-resolution burst mode observations during 16:48:37.604–16:48:37.645 UT. There was also a strong (~ 80 mV) ESW at 16:48:37.620 UT. These waves occur in the separatrix regions close to the EDR. So, Juno was likely in the separatrix region during 16:48:37.604–16:48:37.645 UT. Adjacent to this time, JADE estimated the trend in thermal/suprathermal electron flux and partial PAD around $\sim 16:48:36$ – $16:48:37$ UT and $\sim 16:48:37$ – $16:48:38$ UT from a series of discrete measurements of pitch angles at different energies. A slight increase in electron flux is seen below 1 keV around the later time. Pitch angle observations around 16:48:36–16:48:37 UT indicate a nearly field-aligned distribution expected to be observed in the combined sampling of inflow and outflow region. The PAD changed to a highly field-aligned distribution including a possible jet around 16:48:37–16:48:38 UT indicating JADE was sampling the separatrix region. From JEDI observations, we see an isotropic PAD with slight enhancement in flux in the high energy electrons around $\sim 16:48:36.5$ – $16:48:37.5$ UT, which is marked by the blue and black dashed lines in Figures 3c and 3d, suggesting the passing of Juno over the outflow region. From minimum variance analysis, a reversal of the magnetic field (B_{\max} component) was seen at 16:48:37.107 UT. However, the confidence level of the values of B_{\max} and B_{int} are moderate. Depending on the sequence of events recorded by instruments on Juno, we construct one possible illustration (Figure 7) of the Juno trajectory through the vicinity of the reconnection site. Based on Juno's velocity (~ 18.6 km/s) with respect to Ganymede, the width of the separatrix region from the ECH wave duration (760 μ s) is of the order of 10s of meters. It is to be remembered that the time stamps mentioned here for particle data cannot be used to pinpoint a time with absolute accuracy, they are only indicative of particle behavior around that time. The reconnection site matches the predicted magnetopause crossing from Duling et al. (2022) within 20 s. The

predicted magnetopause crossing is reasonably close to the observed one at 16:50 as reported by Kurth et al. (2022). Alfvén wing reconnection in this region is also likely (Burkholder et al., 2024).

4. Conclusions

This study is the first report of a magnetic reconnection in the wake region of Ganymede's magnetosphere seen by waves, particles, and magnetic field instruments on Juno. Considering the Juno trajectory during PJ-34 (Figure 1) and the permanently favorable magnetic field and the Alfvén wings orientation, encountering the magnetic reconnection event was not surprising. The event reported here was not across the primary tail current sheet but happened to be across a secondary reconnecting current sheet within the turbulent wake region. Complementary observations from both waves and particle instruments were needed to investigate the reconnection site. The Waves instrument is an excellent tool for identifying the separatrix region, but verification of typical particle behaviors from the particle instrument is needed to identify the inflow/outflow regions. The direction of the magnetic field can indicate the likely trajectory of Juno around the reconnection site. Here we presented all the evidence of a close encounter with a reconnection site using waves, particles, and magnetic field data. It is worth reiterating that this study depended on intermittent high-resolution data from various instruments on Juno. High-resolution continuous data during such microscopic phenomena will be helpful for a complete understanding in the future and missions like JUICE (Grasset et al., 2013) may shed more light on such events.

Data Availability Statement

The Waves burst data sets analyzed during the current study are available in the NASA Planetary Data System repository (Kurth & Piker, 2024). The magnetometer data sets analyzed during the current study are available in the NASA Planetary Data System repository (Connerney, 2024). The high-energy particle data sets analyzed during the current study are available in the NASA Planetary Data System repository (Mauk, 2024). The low/medium-energy particle data sets analyzed during the current study are available in the NASA Planetary Data System repository (Allegrini et al., 2024).

Acknowledgments

The research at the University of Iowa is supported by NASA through Contract 699041X with Southwest Research Institute. S.D. has received funding from the European Research Council (ERC) under the European Union's Horizon2020 research and innovation program (Grant agreement No. 884711). We acknowledge the use of the Space Physics Data Repository at the University of Iowa supported by the Roy J. Carver Charitable Trust. Figure 5b used in this article is reprinted from Li et al. (2020) (Figure 4f) published in "Nature Communications" under a Creative Commons license.

References

- Allegrini, F., Bagenal, F., Ebert, R. W., Louarn, P., McComas, D. J., Szalay, J. R., et al. (2022). Plasma observations during the 7 June 2021 Ganymede flyby from the Jovian Auroral Distributions Experiment (JADE) on Juno. *Geophysical Research Letters*, *49*(23), e2022GL098682. <https://doi.org/10.1029/2022GL098682>
- Allegrini, F., Wilson, R. J., Ebert, R. W., & Loeffler, C. (2024). Juno J/SW Jovian auroral distribution calibrated V1.0, JNO-J/SW-JAD-3-calibrated-V1.0. NASA Planetary Data System. <https://doi.org/10.17189/1519715>
- Angelopoulos, V. (2008). The THEMIS mission. *Space Science Reviews*, *141*(1–4), 5–34. <https://doi.org/10.1007/s11214-008-9336-1>
- Asano, Y., Nakamura, R., Shinohara, I., Fujimoto, M., Takada, T., Baumjohann, W., et al. (2008). Electron flat-top distributions around the magnetic reconnection region. *Journal of Geophysical Research*, *113*(A1), A01207. <https://doi.org/10.1029/2007JA012461>
- Birn, J., Drake, J. F., Shay, M. A., Rogers, B. N., Denton, R. E., Hesse, M., et al. (2001). Geospace Environmental Modeling (GEM) magnetic reconnection challenge. *Journal of Geophysical Research*, *106*(A3), 3715–3719. <https://doi.org/10.1029/1999JA900449>
- Biskamp, D. (2000). Magnetic reconnection in plasmas. In *Cambridge monographs on plasma physics*. Cambridge University Press.
- Borg, A. L., Taylor, M. G. G. T., & Eastwood, J. P. (2012). Electron pitch angle distribution during magnetic reconnection diffusion region observations in the Earth's magnetotail. *Annals of Geophysics*, *30*(1), 109–117. <https://doi.org/10.5194/angeo-30-109-2012>
- Burch, J. L., Moore, T. E., Torbert, R. B., & Giles, B. L. (2016). Magnetospheric multiscale overview and science objectives. *Space Science Reviews*, *199*(1–4), 5–21. <https://doi.org/10.1007/s11214-015-0164-9>
- Burkholder, B. L., Chen, L.-J., Sarantos, M., Gershman, D. J., Argall, M. R., Chen, Y., et al. (2024). Global magnetic reconnection during sustained sub-Alfvénic Solar wind driving. *Geophysical Research Letters*, *51*(6), e2024GL108311. <https://doi.org/10.1029/2024GL108311>
- Cattell, C., Dombeck, J., Wygant, J., Drake, J. F., Swisdak, M., Goldstein, M. L., et al. (2005). Cluster observations of electron holes in association with magnetotail reconnection and comparison to simulations. In *Journal of geophysical research: Space physics* (Vol. 110(A1)). American Geophysical Union (AGU). <https://doi.org/10.1029/2004ja010519>
- Chen, L. J., Bessho, N., Lefebvre, B., Vaith, H., Fazakerley, A., Bhattacharjee, A., et al. (2008). Evidence of an extended electron current sheet and its neighboring magnetic island during magnetotail reconnection. *Journal of Geophysical Research*, *113*(A12), A12213. <https://doi.org/10.1029/2008JA013385>
- Clark, G., Kollmann, P., Mauk, B. H., Paranicas, C., Haggerty, D., Rymer, A., et al. (2022). Energetic charged particle observations during Juno's close flyby of Ganymede. *Geophysical Research Letters*, *49*(23), e2022GL098572. <https://doi.org/10.1029/2022GL098572>
- Collinson, G., Paterson, B., Bard, C., Dorelli, J., Glocer, A., Sarantos, M., & Wilson, R. (2018). New results from Galileo's first flyby of Ganymede: Reconnection-driven flows at the low-latitude magnetopause boundary, crossing the cusp, and icy ionospheric escape. *Geophysical Research Letters*, *45*(8), 3382–3392. <https://doi.org/10.1002/2017GL075487>
- Connerney, J. E. P. (2024). Juno mag calibrated data J V1.0, JNO-J-3-FGM-CAL-V1.0. NASA Planetary Data System. <https://doi.org/10.17189/1519711>
- Connerney, J. E. P., Bann, M., Bjarno, J. B., Denver, T., Espley, J., Jorgensen, J. L., et al. (2017). The Juno magnetic field investigation. *Space Science Reviews*, *213*(1–4), 39–138. <https://doi.org/10.1007/s11214-017-0334-z>

- Deng, X. H., Matsumoto, H., Kojima, H., Mukai, T., Anderson, R. R., Baumjohann, W., et al. (2004). Geotail encounter with reconnection diffusion region in the Earth's magnetotail: Evidence of multiple X lines collisionless reconnection? *Journal of Geophysical Research*, *109*, A05206. <https://doi.org/10.1029/2004JA010632>
- Dorelli, J., & Birn, J. (2003). Whistler-mediated magnetic reconnection in large systems: Magnetic flux pileup and the formation of thin current sheets. *Journal of Geophysical Research*, *108*(A3), 1133. <https://doi.org/10.1029/2001JA009180>
- Dorelli, J. C., Glocer, A., Collinson, G., & Tóth, G. (2015). The role of the Hall effect in the global structure and dynamics of planetary magnetospheres: Ganymede as a case study. *Journal of Geophysical Research: Space Physics*, *120*(7), 5377–5392. <https://doi.org/10.1002/2014JA020951>
- Duling, S., Saur, J., Clark, G., Allegrini, F., Greathouse, T., Gladstone, R., et al. (2022). Ganymede MHD model: Magnetospheric context for Juno's PJ34 flyby. *Geophysical Research Letters*, *49*(24), e2022GL101688. <https://doi.org/10.1029/2022GL101688>
- Ebert, R. W., Allegrini, F., Bagenal, F., Bolton, S. J., Connerney, J. E. P., Clark, G., et al. (2017). Accelerated flows at Jupiter's magnetopause: Evidence for magnetic reconnection along the dawn flank. *Geophysical Research Letters*, *44*(10), 4401–4409. <https://doi.org/10.1002/2016GL072187>
- Ebert, R. W., Fuselier, S. A., Allegrini, F., Bagenal, F., Bolton, S. J., Clark, G., et al. (2022). Evidence for magnetic reconnection at Ganymede's upstream magnetopause during the PJ34 Juno flyby. *Geophysical Research Letters*, *49*(23), e2022GL099775. <https://doi.org/10.1029/2022GL099775>
- Egedal, J., Le, A., Katz, N., Chen, L. J., Lefebvre, B., Daughton, W., & Fazakerley, A. (2010). Cluster observations of bidirectional beams caused by electron trapping during antiparallel reconnection. *Journal of Geophysical Research*, *115*(A3), A03214. <https://doi.org/10.1029/2009JA014650>
- Egedal, J., Øieroset, M., Fox, W., & Lin, R. P. (2005). In situ discovery of an electrostatic potential, trapping electrons and mediating fast reconnection in the Earth's magnetotail. *Physical Review Letters*, *94*(2), 025006. <https://doi.org/10.1103/PhysRevLett.94.025006>
- Ergun, R. E., Pathak, N., Usanova, M. E., Qi, Y., Vo, T., Burch, J. L., et al. (2022). Observation of magnetic reconnection in a region of strong turbulence. *ApJL*, *935*(1), L8. <https://doi.org/10.3847/2041-8213/ac81d4>
- Eriksson, E., Vaivads, A., Graham, D. B., Divin, A., Khotyaintsev, Y. V., Yordanova, E., et al. (2018). Electron energization at a reconnecting magnetosheath current sheet. *Geophysical Research Letters*, *45*(16), 8081–8090. <https://doi.org/10.1029/2018GL078660>
- Escoubet, C. P., Fehring, M., & Goldstein, M. (2001). The cluster mission. *Annals of Geophysics*, *19*(10/12), 1197–1200. <https://doi.org/10.5194/angeo-19-1197-2001>
- Fatemi, S., Poppe, A. R., Khurana, K. K., Holmström, M., & Delory, G. T. (2016). On the formation of Ganymede's surface brightness asymmetries: Kinetic simulations of Ganymede's magnetosphere. *Geophysical Research Letters*, *43*(10), 4745–4754. <https://doi.org/10.1002/2016GL068363>
- Fuselier, S. A., Frahm, R., Lewis, W. S., Masters, A., Mukherjee, J., Petrinc, S. M., & Sillanpaa, I. J. (2014). The location of magnetic reconnection at Saturn's magnetopause: A comparison with Earth. *Journal of Geophysical Research: Space Physics*, *119*(4), 2563–2578. <https://doi.org/10.1002/2013JA019684>
- Fuselier, S. A., Vines, S. K., Burch, J. L., Petrinc, S. M., Trattner, K. J., Cassak, P. A., et al. (2017). Large-scale characteristics of reconnection diffusion regions and associated magnetopause crossings observed by MMS. *Journal of Geophysical Research: Space Physics*, *122*(5), 5466–5486. <https://doi.org/10.1002/2017JA0240>
- Grasset, O., Dougherty, M., Coustenis, A., Bunce, E., Erd, C., Titov, D., et al. (2013). Jupiter ICy moons explorer (JUICE): An ESA mission to orbit Ganymede and to characterise the Jupiter system. *Planetary and Space Science*, *78*(2013), 1–21. <https://doi.org/10.1016/j.pss.2012.12.002>
- Gurnett, D. A., Kurth, W. S., Roux, A., Bolton, S. J., & Kennel, C. F. (1996). Evidence for a magnetosphere at Ganymede from plasma-wave observations by the Galileo spacecraft. *Nature*, *384*(6609), 535–537. <https://doi.org/10.1038/384535a0>
- Hansen, C. J., Bolton, S., Sulaiman, A. H., Duling, S., Bagenal, F., Brennan, M., et al. (2022). Juno's close encounter with Ganymede—An overview. *Geophysical Research Letters*, *49*(23), e2022GL099285. <https://doi.org/10.1029/2022GL099285>
- Hubbard, R. F., Birmingham, T. J., & Hones, J. E. W. (1979). Magnetospheric electrostatic emissions and cold plasma densities. *Journal of Geophysical Research*, *84*(A10), 5828–5838. <https://doi.org/10.1029/JA084iA10p05828>
- Jia, X., & Kivelson, M. G. (2021). The magnetosphere of Ganymede. In *Magnetospheres in the solar system* (pp. 557–573). American Geophysical Union (AGU). <https://doi.org/10.1002/9781119815624.ch35>
- Karimabadi, H., Dorelli, J., Roytershteyn, V., Daughton, W., & Chacón, L. (2011). Flux pile-up in collisionless magnetic reconnection: Bursty interaction of large flux ropes. *Physical Review Letters*, *107*(2), 025002. <https://doi.org/10.1103/physrevlett.107.025002>
- Kaweeyanun, N., Masters, A., & Jia, X. (2020). Favorable conditions for magnetic reconnection at Ganymede's upstream magnetopause. *Geophysical Research Letters*, *47*(6), e2019GL086228. <https://doi.org/10.1029/2019GL086228>
- Khotyaintsev, Y. V., Graham, D. B., Norgren, C., & Vaivads, A. (2019). Collisionless magnetic reconnection and waves: Progress review. *Frontiers in Astronomy and Space Sciences*, *6*, 70. <https://doi.org/10.3389/fspas.2019.00070>
- Khotyaintsev, Y. V., Vaivads, A., André, M., Fujimoto, M., Retinò, A., & Owen, C. J. (2010). Observations of slow electron holes at a magnetic reconnection site. *Physical Review Letters*, *105*(16), 165002. <https://doi.org/10.1103/PhysRevLett.105.165002>
- Kivelson, M. G., Khurana, K. K., Russell, C. T., Walker, R. J., Warnecke, J., Coroniti, F. V., et al. (1996). Discovery of Ganymede's magnetic field by the Galileo spacecraft. *Nature*, *384*(6609), 537–541. <https://doi.org/10.1038/384537a0>
- Kivelson, M. G., Khurana, K. K., & Volwerk, M. (2002). The permanent and inductive magnetic moments of Ganymede. *Icarus*, *157*(2), 507–522. <https://doi.org/10.1006/icar.2002.6834>
- Kurth, W. S., Hospodarsky, G. B., Kirchner, D. L., Mokrzycki, B. T., Averkamp, T. F., Robison, W. T., et al. (2017). The Juno waves investigation. *Space Science Reviews*, *213*(1–4), 347–392. <https://doi.org/10.1007/s11214-017-0396-y>
- Kurth, W. S., & Piker, C. W. (2024). *Juno eJIS/SS waves calibrated burst full resolution V2.0, JNO-EJIS-WAV-3-CDR-BSTFULL-V2.0*. NASA Planetary Data System. <https://doi.org/10.17189/1522461>
- Kurth, W. S., Sulaiman, A. H., Hospodarsky, G. B., Menietti, J. D., Mauk, B. H., Clark, G., et al. (2022). Juno plasma wave observations at Ganymede. *Geophysical Research Letters*, *49*(23), e2022GL098591. <https://doi.org/10.1029/2022GL098591>
- Li, W. Y., Graham, D. B., Khotyaintsev, Y. V., Vaivads, A., André, M., Min, K., et al. (2020). Electron Bernstein waves driven by electron crescents near the electron diffusion region. *Nature Communications*, *11*(1), 141. <https://doi.org/10.1038/s41467-019-13920-w>
- Li, X., Wang, R., Lu, Q., Russell, C. T., Lu, S., Cohen, I. J., et al. (2022). Three-dimensional network of filamentary currents and super-thermal electrons during magnetotail magnetic reconnection. *Nature Communications*, *13*(1), 3241. <https://doi.org/10.1038/s41467-022-31025-9>
- Masters, A. (2017). Model-based assessments of magnetic reconnection and Kelvin-Helmholtz instability at Jupiter's magnetopause. *Journal of Geophysical Research: Space Physics*, *122*, 11–154. <https://doi.org/10.1002/2017JA024736>
- Mauk, B. (2024). *Jedi calibrated (CDR) data JNO J JED 3 CDR V1.0*. NASA Planetary Data System. <https://doi.org/10.17189/1519173>

- Mauk, B. H., Haggerty, D. K., Jaskulek, S. E., Schlemm, C. E., Brown, L. E., Cooper, S. A., et al. (2017). The Jupiter Energetic Particle Detector Instrument (JEDI) investigation for the Juno mission. *Space Science Reviews*, *213*(1), 289–346. <https://doi.org/10.1007/s11214-013-0025-3>
- McComas, D. J., Alexander, N., Allegrini, F., Bagenal, F., Beebe, C., Clark, G., et al. (2017). The Jovian Auroral Distributions Experiment (JADE) on the Juno mission to Jupiter. *Space Science Reviews*, *213*(1–4), 547–643. <https://doi.org/10.1007/s11214-013-9990-9>
- Nagai, T., Shinohara, I., Fujimoto, M., Hoshino, M., Saito, Y., Machida, S., & Mukai, T. (2001). Geotail observations of the hall current system: Evidence of magnetic reconnection in the magnetotail. *Journal of Geophysical Research*, *106*(A11), 25929–25949. <https://doi.org/10.1029/2001JA900038>
- Nan, J., Huang, K., Lu, Q., Lu, S., Wang, R., Xie, J., et al. (2022). Formation of the electron inflow along the separatrices during collisionless magnetic reconnection. *Journal of Geophysical Research: Space Physics*, *127*(5), e2021JA029996. <https://doi.org/10.1029/2021JA029996>
- Øieroset, M., Lin, R. P., Phan, T. D., Larson, D. E., & Bale, S. D. (2002). Evidence for electron acceleration up to ~300 keV in the magnetic reconnection diffusion region of Earth's magnetotail. *Physical Review Letters*, *89*(19), 195001. <https://doi.org/10.1103/PhysRevLett.89.195001>
- Paschmann, G., & Daly, P. W. (1998). *Analysis methods for multi-spacecraft data* (Vol. 1). ESA Publications Division.
- Paschmann, G., Øieroset, M., & Phan, T. (2013). In-situ observations of reconnection in space. *Space Science Reviews*, *178*(2–4), 385–417. <https://doi.org/10.1007/s11214-012-9957-2>
- Phan, T. D., Shay, M. A., Gosling, J. T., Fujimoto, M., Drake, J. F., Paschmann, G., et al. (2013). Electron bulk heating in magnetic reconnection at Earth's magnetopause: Dependence on the inflow Alfvén speed and magnetic shear. *Geophysical Research Letters*, *40*(17), 4475–4480. <https://doi.org/10.1002/grl.50917>
- Retinó, A., Vaivads, A., André, M., Sahraoui, F., Khotyaintsev, Y., Pickett, J. S., et al. (2006). Structure of the separatrix region close to a magnetic reconnection X-line: Cluster observations. *Geophysical Research Letters*, *33*(6), L06101. <https://doi.org/10.1029/2005GL024650>
- Romanelli, N., DiBraccio, G. A., Modolo, R., Connerney, J. E. P., Ebert, R. W., Martos, Y. M., et al. (2022). Juno magnetometer observations: Comparisons with a global hybrid simulation and indications of magnetopause reconnection. *Geophysical Research Letters*, *49*(23), e2022GL099545. <https://doi.org/10.1029/2022gl099545>
- Sonnerup, B. (1979). Magnetic field reconnection. In L. J. Lanzerotti, C. F. Kennel, & E. N. Parker (Eds.), *Solar system plasma physics* (Vol. 1, pp. 45–108). North-Holland Publishing Company.
- Sonnerup, B., & Cahill, L. J. (1967). Magnetopause structure and attitude from explorer 12 observations. *Journal of Geophysical Research*, *72*(1), 171–183. <https://doi.org/10.1029/JZ072i001p00171>
- Terasawa, T. (1983). Hall current effect on tearing mode instability. In *Geophysical research letters* (Vol. 10(6), 475–478). American Geophysical Union (AGU). <https://doi.org/10.1029/gl10i006p00475>
- Umeda, T. (2007). Numerical study of electrostatic electron cyclotron harmonic waves due to Maxwellian ring velocity distributions. *Earth Planets and Space*, *59*(11), 1205–1210. <https://doi.org/10.1186/BF03352068>
- Vaivads, A., Khotyaintsev, Y., André, M., Retinó, A., Buchert, S., Rogers, B., et al. (2004). Structure of the magnetic reconnection diffusion region from four-spacecraft observations. *Physical Review Letters*, *93*(10), 105001. <https://doi.org/10.1103/PhysRevLett.93.105001>
- Viberg, H., Khotyaintsev, Y. V., Vaivads, A., André, M., & Pickett, J. S. (2013). Mapping HF waves in the reconnection diffusion region. *Geophysical Research Letters*, *40*(6), 1032–1037. <https://doi.org/10.1002/grl.50227>
- Webster, J. M., Burch, J. L., Reiff, P. H., Daou, A. G., Genestreti, K. J., Graham, D. B., et al. (2018). Magnetospheric multiscale dayside reconnection electron diffusion region events. *Journal of Geophysical Research: Space Physics*, *123*(6), 4858–4878. <https://doi.org/10.1029/2018JA025245>